IEEE Access
Multidisciplinary | Rapid Review | Open Access Journal

Received 22 September 2023, accepted 27 October 2023, date of publication 1 November 2023,
date of current version 7 November 2023.

Digital Object Identifier 10.1109/ACCESS.2023.3329166

RESEARCH ARTICLE

Online MTPA Control of IPM Motor Using NN-Based Perturb and Observe Algorithm

LINFENG SUN[1,2], JIAWEI GUO[1], TAKAHIRO KAWAGUCHI[1], (Associate Member, IEEE), SEIJI HASHIMOTO[1], (Member, IEEE), AND WEI JIANG[2]

[1]Division of Electronics and Informatics, Gunma University, Kiryu, Gunma 376-8515, Japan
[2]Department of Electrical Engineering, Yangzhou University, Yangzhou 225127, China

Corresponding author: Seiji Hashimoto (hashimotos@gunma-u.ac.jp)

This work was supported in part by JSPS KAKENHI under Grant JP22K04150.

ABSTRACT In commercial electrical equipment, interior permanent magnet (IPM) synchronous motors undergo variations in temperature and parameters under different operating conditions. Conventional maximum torque per ampere (MTPA) control using fixed parameters lacks accurate motor parameter information, which can negatively impact the operating efficiency of electrical equipment. To address the above problem, this paper proposes a simple online MTPA control method without motor parameters. To approximate the interface structure of the conventional MTPA controller, a back propagation neural network (BP-NN) adjuster with a space vector decomposer is designed as the MTPA controller. Moreover, by leveraging the similarity between the loss function of the BP-NN and the stator current representing the efficiency of the IPM motor, the teacher signal is cleverly chosen to update the parameters of the BP-NN online. In the discrete domain, the motion mechanism of the proposed method is analyzed and characterized by the perturb & observe technique. Compared to the conventional MTPA control using fixed parameters, the feasibility and high efficiency of the proposed method for copper-loss-minimization control were validated in the simulation. The feasibility of the proposed method was further validated in simulated scenarios involving sudden changes in torque and speed. Furthermore, the transient characteristics of the output stator current were analyzed. Overall, the proposed method can achieve true online MTPA control without motor parameters.

INDEX TERMS Interior permanent magnet synchronous motor, field-oriented control, maximum torque per ampere control, back propagation neural network, loss function, perturb and observe.

I. INTRODUCTION

With rapid increasing usage of synchronous motors in various industries, synchronous motors have become more popular and are expanded into various mechanical structures by scholars. Among them, due to high power density, wide speed range, strong reliability, low-noise operation and high efficiency [1], [2], interior permanent magnet (IPM) synchronous motors are being widely used in the field of electric vehicles, industrial drives, industrial automation and household appliances, etc. However, a significant portion of the global electricity consumption comes from electric motors used in applications, such as pumps, fans and compressors [3]. In these applications, IPM motors mostly operate under constant load torque. Therefore, it is very important to improve the operating efficiency of IPM motors at steady state.

In synchronous motors, copper losses typically dominate over iron losses, and the evaluation of iron losses is frequently overlooked [4]. Therefore, in IPM motor control technologies, maximum torque per ampere (MTPA) control methods are often used to improve the efficiency of IPM motors and provide maximum torque or minimum stator current to minimize copper losses. Based on the field oriented control (FOC) technology and the equivalent model of IPM motor in the direct-quadrature (dq) frame, the conventional offline method for implementing MTPA control is to calculate MTPA equations, under the assumption of stable and known motor parameters [5], [6]. However, due to steel saturation, cross-saturation and flux linkage affected by

The associate editor coordinating the review of this manuscript and approving it for publication was Junhua Li.

temperature, motor parameters vary depending on different operating conditions. The d- and q-axis inductances, which are dependent on the stator current, can decrease by up to 50% due to steel saturation [7]; high temperatures of the stator can cause flux linkage variations of 10% to 20% [8], [9], [10], and magnet degradation can decrease the flux linkage by 15% [11]. In order to improve the control algorithm, researchers have proposed various offline or online MTPA methods for parameter calculation, parameter estimation and parameter-free control, etc [10], [12].

Generally, offline methods heavily rely on prior information that includes functions or look-up tables for approximating motor parameters or the MTPA curve [13], [14], [15]. Moreover, the processing of acquiring information can only be done for a specific motor or a limited number of motors during the development stage. In contrast, online control methods enable the motor to operate at the MTPA point without the need for prior knowledge of parameters or the MTPA curve. This is particularly applicable in the development of industrial or household general-purpose products sold in large quantities. Parameter estimation methods and extremum seeking methods are two highly popular research directions within online methods.

The purpose of parameter estimation methods is to online obtain accurate motor parameters using various online estimation techniques during motor operation. These methods can enhance offline methods with accurately estimated parameters. The authors in [16] and [18] proposed the estimation of motor parameters by combining recursive least squares with rich enough motor data in real-time. The proposal [17] identified d- and q-axis inductances by model reference adaptive system (MRAS) based on the Popov stability criterion. However, parameter estimation methods not only require complex estimation formulas but also need to consider observability issues caused by rank deficiency [19]. Complex estimation formulas, such as those involving the calculation of numerous square roots, impose higher demands on processors like DSPs in practical applications and are not easy to implement; rank deficiency issues can prevent parameter estimation methods from observing all parameters, including flux linkage [17].

To overcome these problems, extremum seeking methods [11], [20], [21], [22], [23], [24], [25], [26] that do not require motor parameters and analytical motor models are being considered. These model-free methods interact with the motor online in a closed-loop manner and apply a perturbation to the stator current space vector reference for probing purposes; based on the response to such stimulus, the operating point is dynamically adjusted in real-time to track the MTPA point at constant torque or current [10], [12]. Therefore, extremum seeking methods particularly rely on the situation where the load torque or stator current space vector remains constant. This aligns perfectly with the applications considered in this paper, where IPM motors mostly operate under constant load torque.

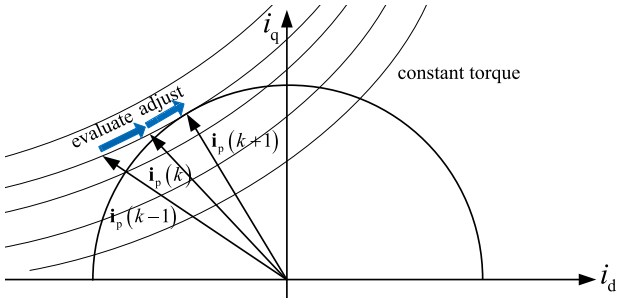

FIGURE 1. Operating principle of P&O methods.

As a branch, signal injection methods introduce a relatively high frequency small signal to the current angle, and detect torque oscillation by processing the measured speed or estimated active power at constant stator current [20], [21]; they can also introduce a relatively low frequency small signal to the current angle, and detect stator current oscillation at constant torque [22]. Evidently, high frequency injection methods are not suitable for the situation described in this paper; low frequency injection methods can lead to undesirable noise. Recently, as an improvement, a new method called virtual signal injection can be used to detect the MTPA trajectory by injecting virtual signals [23], [24]. However, this method has several limitations, such as implicit angle errors and sensitivity to the variation of stator resistance, and it is not recommended.

Fortunately, perturb & observe (P&O) methods, as another extremum seeking algorithms, can be used to track the MTPA point online without the need for motor parameters, analytical motor models, or being affected by signal injection. P&O methods are easy to implement. These methods just evaluate the effect of operating point discrete variations and then make further adjustments to the operating point, as shown in Fig. 1. In practical applications, an enhanced MTPA controller strategy based on the P&O technology in [25] is used to achieve robust high-efficient operation of the sensorless IPM motor, and does not require motor parameters; in [26], the propsoed MTPA automatic search strategy based on the P&O technology is capable of providing a reliable and fast response to operating point variation. Moreover, the proposal [11] has already applied the improved P&O algorithm in the drives with commercial reciprocating compressors. Finally, after a careful analysis of the advantages and disadvantages of all the aforementioned methods, the P&O technology is used to guide the design of the proposed online MTPA method.

In addition, the development of artificial intelligence technology provides numerous new techniques for the field of motor drive [27]. For example, in [28], the radial basis function neural network is combined to optimize and reduce the torque ripple of an IPM motor. In [29], a new wavelet fuzzy neural network is used to enhance the robustness of the speed integral-proportional controller. In this paper, combined with back propagation neural network (BP-NN)

technology, an online MTPA control of IPM motor using NN-based P&O algorithm is proposed.

The rest of this paper is organized as follows. In section II, the equivalent model of IPM motor for FOC and the conventional MTPA with fixed parameters are introduced. In section III, the design and motion mechanism of the proposed online MTPA control of IPM motor using NN-based P&O algorithm are presented. In section IV, compared to the conventional MTPA and optimal MTPA, the feasibility of the proposed method is analyzed. In section V, the conclusion of the proposed method is presented.

II. MODELING AND CONVENTIONAL MTPA CONTROL OF IPM MOTOR

A. EQUIVALENT MODELING OF IPM MOTOR

In general, d-q axis equivalent model of IPM motor can be used for FOC and to easily analyze three-phase motor characteristics as a DC motor. It is easy to design MTPA control method by FOC technology in the vector space. By using power-variant Park coordinate transformation, the 3-phase IPM motor model can be reduced to two dimensions from abc coordinate frame. Voltage equations, electromagnetic torque equation and mechanical motion equation of IPM motor in dq rotating coordinate frame can be defined as (1), (2) and (3), separately. The relationship between mechanical angular speed and electrical angular speed is shown in (4).

$$\begin{bmatrix} u_d \\ u_q \end{bmatrix} = R_s \begin{bmatrix} i_d \\ i_q \end{bmatrix} + \begin{bmatrix} R_s + L_d \frac{d}{dt} & -L_q \omega_e \\ L_d \omega_e & R_s + L_q \frac{d}{dt} \end{bmatrix} \begin{bmatrix} i_d \\ i_q \end{bmatrix} + \begin{bmatrix} 0 \\ \omega_e \psi_f \end{bmatrix} \tag{1}$$

$$T_e = \frac{3}{2} p_n i_q \left(i_d \left(L_d - L_q \right) + \psi_f \right) \tag{2}$$

$$J \frac{d\omega_m}{dt} = T_e - T_L - B\omega_m \tag{3}$$

$$\omega_e = p_n \omega_m \tag{4}$$

where L_d and L_q are the d- and q-axis stator inductances, R_s is the resistance of the stator winding, u_d and u_q are the d- and q-axis stator voltage, i_d and i_q are the d- and q-axis stator current, ψ_f is the permanent magnet flux linkage, p_n is the polar pairs, J is the moment of inertia, T_e and T_L are the electromagnetic and the load torques, B is the viscous friction coefficient, ω_m and ω_e are the mechanical and the electrical angular speeds. The copper loss power p_c evaluating the efficiency of MTPA control can be expressed as (5). At constant torque, lower copper loss power indicates the higher efficiency of the copper-loss-minimization control.

$$p_c = {i_p}^2 R_s = \left\| \mathbf{i}_{dq} \right\|^2 R_s = \left({i_d}^2 + {i_q}^2 \right) R_s \tag{5}$$

where stator current i_p is the magnitude of stator current space vector $\mathbf{i}_{dq}$.

B. CONVENTIONAL MTPA CONTROL WITH FIXED PARAMETERS

Based on Lagrange's theorem, at constant torque $T_e{}^*$, the Lagrangian expression $L(i_d, i_q, \lambda)$ can be defined as (6) by substituting torque in (2) [12]. When all three partial derivatives meet (7), the conventional MTPA condition can be determined.

$$L\left(i_d, i_q, \lambda\right) = \sqrt{{i_d}^2 + {i_q}^2} + \lambda \left(T_e - T_e{}^* \right) \tag{6}$$

$$\frac{\partial L}{\partial i_d} = 0, \quad \frac{\partial L}{\partial i_q} = 0, \quad \frac{\partial L}{\partial \lambda} = 0 \tag{7}$$

where λ is a Lagrangian multiplier. Assuming that the IPM motor parameters which are d- and q-axis inductances and permanent magnet flux linkage, are stable and known, the minimum stator current space vector reference which represents the MTPA point can be expressed as (8) and (9).

$$\theta_i{}^* = \arccos \left(\frac{-\psi_f + \sqrt{{\psi_f}^2 + 8\left(L_d - L_q\right)^2 {i_p}^{*2}}}{4\left(L_d - L_q\right) i_p{}^*} \right) \tag{8}$$

$$i_d{}^* = -i_p{}^* \sin\theta_i{}^*, \; i_q{}^* = i_p{}^* \cos\theta_i{}^* \tag{9}$$

where $\theta_i{}^*$ and $i_p{}^*$ can be considered as the stator current angle reference and stator current reference at the MTPA point in the conventional method, respectively. Combining IPM motor equations (1), (2) and (3), and MTPA condition (8) and (9), the conventional MTPA control method in the sensorless drive system can be obtained in Fig. 2.

The control aspect of the conventional method mainly consists of a speed controller, an MTPA controller using fixed parameters, a current controller, a rotating coordinate transformation/inverse transformation unit and a PWM modulator, etc. Obviously, the conventional method with fixed parameters cannot achieve optimal MTPA control due to the variation of motor parameters and the lack of real-time and accurate parameter information [7], [8], [9], [10], [11].

III. PROPOSED MTPA CONTROL USING NN-BASED P&O ALGORITHM

To solve the deficiency of the conventional MTPA control with fixed parameters and reduce control complexity, in Fig. 3, an online MTPA controller using NN-based P&O algorithm which can also be called a parameter-free online NN-based MTPA controller is proposed. It can replace the conventional MTPA controller due to BP-NN's excellent online iteration and convergence capabilities. The proposed controller consists of an NN-based MTPA angle calculation unit and a space vector decomposition unit following (9). Among them, the design of the angle calculation unit is mainly from two aspects: NN structure and loss function. And the motion mechanism of the proposed network needs to be analyzed. The space vector decomposition unit is shown in Fig. 4(c).

A. ARCHITECTURE OF THE PROPOSED NN-BASED MTPA CONTROLLER

1) NN STRUCTURE

The MTPA angle calculation unit is a BP-NN which consists of one input layer, two hidden layers and one output layer, shown as Fig. 4(a). The input layer contains two input signals

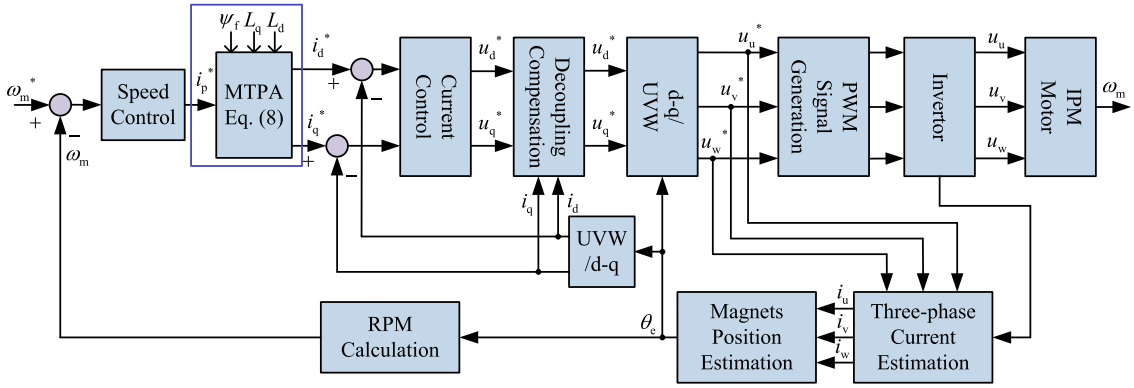

FIGURE 2. Block diagram of the conventional MTPA control method in the sensorless drive system.

which are output $i_p{}^*(k)$ of the speed controller and actual stator current $i_p(k)$ of the IPM motor. The output $i_p{}^*(k)$ of the speed controller can be described in (10). The output signal is the current angle reference $\theta_i{}^*(k)$. The number of hidden layers of the NN was two because of its stronger approximation ability than a one-hidden NN [30]. Using the trial-and-error method, the number of neurons in each hidden layer was determined to be ten by gradually increasing the number of neurons and evaluating them step by step. The activation function of hidden layers is the commonly used hyperbolic tangent function tanh, and the neurons of the output layer has no activation function and no bias. Theoretically, the teacher signal is the value obtained by dividing stator current difference between $i_p(k)$ and $i_p(k-1)$ by current angle reference difference between $\theta_i{}^*(k-1)$ and $\theta_i{}^*(k-2)$ at time step k.

$$\begin{cases} e(k) = \omega_m{}^*(k) - \omega_m(k) \\ i_p{}^*(k) = i_p{}^*(k-1) + K_p e(k) + K_i T_s (e(k) - e(k-1)) \\ i_p{}^*(k-1) = i_p{}^*(k) \\ e(k-1) = e(k) \end{cases} \tag{10}$$

where $\omega_m{}^*(k)$ is the speed reference, $\omega_m(k)$ is the actual motor speed, $e(k)$ is the error between $\omega_m{}^*(k)$ and $\omega_m(k)$, T_s is the discrete period, K_p and K_i are the proportional and integral coefficients of the PI controller of the speed loop, respectively.

2) LOSS FUNCTION

At time step k, the loss function $L(\theta_i{}^*(k-1))$ used for back propagation and updating parameters of BP-NN in Fig. 4(b) is the stator current space vector magnitude $i_p(k)$. In the loss function, the logic of the proposed teacher signal follows the derivative of the output $i_p(k)$ with respect to the input $\theta_i{}^*(k-1)$. To improve the convergence speed around the gradient point and avoid numerical overflow during calculations, the sign of theoretical teacher signal in (11) is selected as the adopted teacher signal and used in the discrete algorithm. On the other hand, the input-output relationship of the loss function also represents the dynamic relationship of the IPM

TABLE 1. Mapping relationship between IPM motor and BP-NN.

	IPM motor	BP-NN
$L(\theta_i{}^*)$	Relationship between $\theta_i{}^*$ and i_p of IPM motor.	Loss function.
$L_{\min}(\theta_i{}^*)$	MTPA point.	Extreme point of the loss function.

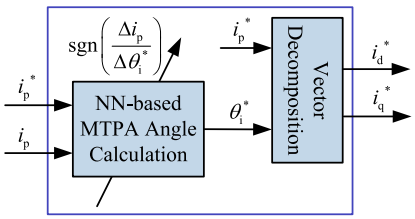

FIGURE 3. Block diagram of the proposed NN-based MTPA controller.

motor at constant torque $T_e{}^*$ in (12) and is consistent with the convex curve in Fig. 5, corresponding to (2). Therefore, the mapping relationship between the IPM motor and BP-NN can be obtained, as shown in Table 1. Coincidentally, the gradient point sought by BP-NN is exactly the efficiency point of the IPM motor, where i_p is the minimum. So, the proposed method is feasible and has MTPA control ability theoretically.

$$\begin{aligned} & sgn\left(\dot{L}\left(\theta_i{}^*(k-1)\right)\right) \\ & = \begin{cases} 1, & i_p(k) - i_p(k-1) > 0, \\ & \theta_i{}^*(k-1) - \theta_i{}^*(k-2) > 0. \\ 1, & i_p(k) - i_p(k-1) < 0, \\ & \theta_i{}^*(k-1) - \theta_i{}^*(k-2) < 0. \\ -1, & i_p(k) - i_p(k-1) > 0, \\ & \theta_i{}^*(k-1) - \theta_i{}^*(k-2) < 0. \\ -1, & i_p(k) - i_p(k-1) < 0, \\ & \theta_i{}^*(k-1) - \theta_i{}^*(k-2) > 0. \\ 0, & otherwise. \end{cases} \\ & f\left(\theta_i{}^*(k-1), i_p(k)\right)_{T_e = T_e{}^*} \end{aligned} \tag{11}$$

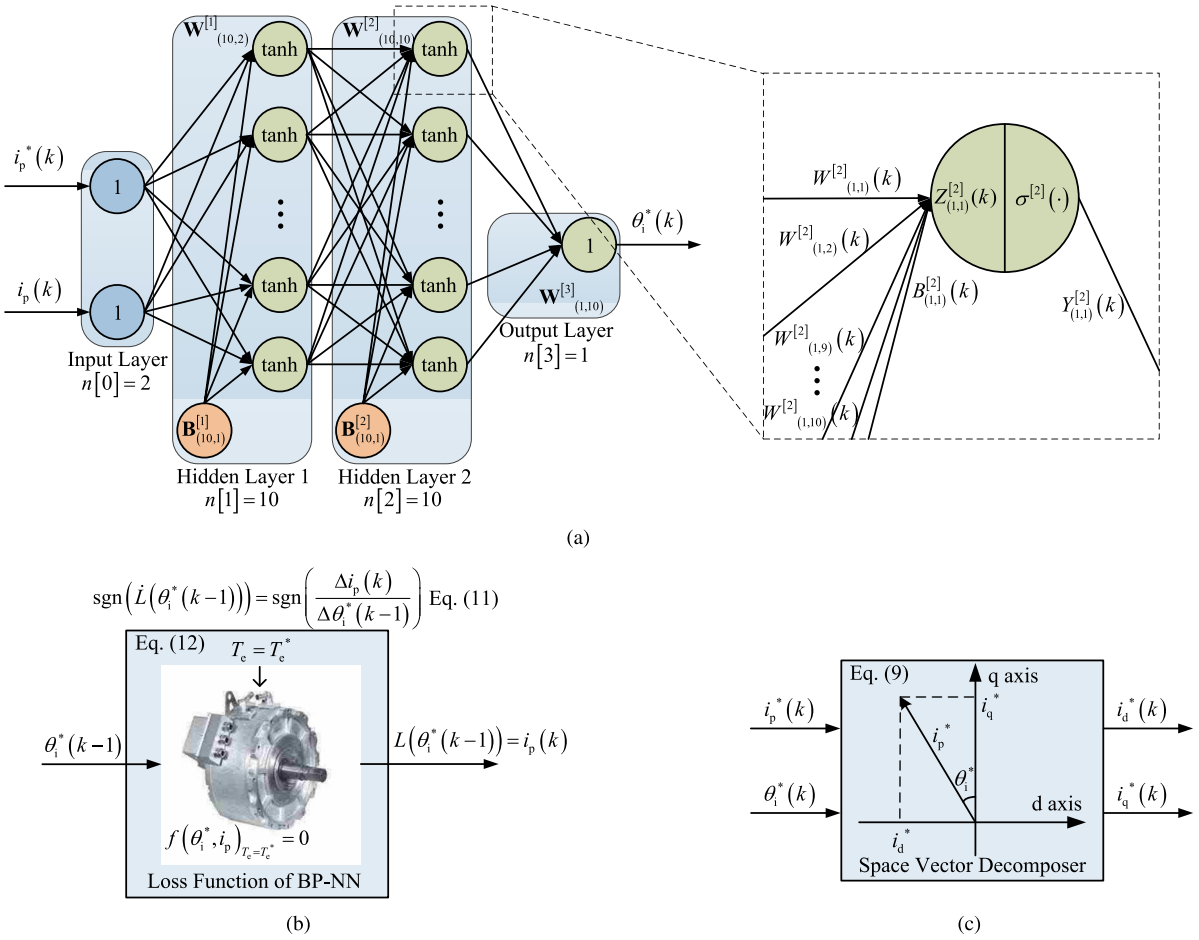

FIGURE 4. Architecture of the proposed NN-based MTPA controller. (a) Structure of the proposed BP-NN. (b) Loss function of the proposed BP-NN. (c) Space vector decomposer.

$$= T_e{}^* - \frac{3}{4} p_n \left(L_q - L_d\right) \left(i_p\left(k\right)\right)^2 \sin\left(2\theta_i{}^*\left(k-1\right)\right) - \frac{3}{2} p_n \psi_f i_p\left(k\right) \cos\left(\theta_i{}^*\left(k-1\right)\right) = 0 \tag{12}$$

3) DISCRETE ALGORITHM

Apparently, the discrete algorithm for processing can be obtained based on the proposed BP-NN. In detail, at time step k, the MTPA tuning algorithm consists of three steps in each iteration, namely back propagation, gradient descent and forward propagation in sequence. Back propagation and gradient descent are specific steps to update the parameters of the BP-NN based on the previous two states and this state; forward propagation using updated parameters is used to adjust the current angle. The back propagation of the i-th layer for calculating the gradient is given as shown in (13) and (14).

$$\begin{cases} d\mathbf{Z}^{[i]}_{(n[i],1)}(k-1) = d\mathbf{Y}^{[i]}_{(n[i],1)}(k-1) \\ = sgn\left(\dot{L}\left(\theta_i{}^*(k-1)\right)\right) \\ d\mathbf{W}^{[i]}_{(n[i],n[i-1])}(k-1) \\ = d\mathbf{Z}^{[i]}_{(n[i],1)}(k-1) \cdot \left(\mathbf{Y}^{[i-1]}_{(n[i-1],1)}(k-1)\right)^T \\ i = 3 \end{cases} \tag{13}$$

$$\begin{cases} d\mathbf{Z}^{[i]}_{(n[i],1)}(k-1) = \left(\mathbf{W}^{[i+1]}_{(n[i+1],n[i])}(k-1)\right)^T \\ \cdot d\mathbf{Z}^{[i+1]}_{(n[i+1],1)}(k-1) \odot \sigma'^{[i]}\left(\mathbf{Z}^{[i]}_{(n[i],1)}(k-1)\right) \\ d\mathbf{W}^{[i]}_{(n[i],n[i-1])}(k-1) \\ = d\mathbf{Z}^{[i]}_{(n[i],1)}(k-1) \cdot \left(\mathbf{Y}^{[i-1]}_{(n[i-1],1)}(k-1)\right)^T \\ d\mathbf{B}^{[i]}_{(n[i],1)}(k-1) = d\mathbf{Z}^{[i]}_{(n[i],1)}(k-1) \\ i = 1, 2 \end{cases} \tag{14}$$

where i indicates the i-th layer, $n[i]$ indicates the size of the i-th layer, the numbers inside parentheses $(n[i], n[i-1])$ indicate the dimension of a vector or matrix, $\mathbf{W}^{[i+1]}_{(n[i+1],n[i])}(k-1)$, $\mathbf{B}^{[i]}_{(n[i],1)}(k-1)$, $\mathbf{Z}^{[i]}_{(n[i],1)}(k-1)$, $\sigma^{[i]}(\cdot)$ and $\mathbf{Y}^{[i]}_{(n[i],1)}(k-1)$ are the weight, bias, activation function's input, activation function and output of the i-th layer, respectively, the symbol $\odot$ is Hadamard product. Then, the gradient descent of the i-th layer for updating weights and biases is given as shown in (15) and (16).

$$\begin{cases} \mathbf{W}^{[i]}_{(n[i],n[i-1])}(k) = \mathbf{W}^{[i]}_{(n[i],n[i-1])}(k-1) \\ -\alpha \cdot d\mathbf{W}^{[i]}_{(n[i],n[i-1])}(k-1) \\ i = 3 \end{cases} \tag{15}$$

$$\begin{cases} \mathbf{W}^{[i]}_{(n[i],n[i-1])}(k) = \mathbf{W}^{[i]}_{(n[i],n[i-1])}(k-1) \\ -\alpha \cdot d\mathbf{W}^{[i]}_{(n[i],n[i-1])}(k-1) \\ \mathbf{B}^{[i]}_{(n[i],1)}(k) = \mathbf{B}^{[i]}_{(n[i],1)}(k-1) \\ -\beta \cdot d\mathbf{B}^{[i]}_{(n[i],1)}(k-1) \\ i = 1, 2 \end{cases} \tag{16}$$

where hyperparameters α and β determine the step size of updating weights and biases. Finally, the forward propagation of the i-th layer for obtaining $\theta_i{}^*(k)$ is given as shown in (17) and (18). The input of the 1st layer and the output of the 3rd layer are described in (19) and (20), respectively.

$$\begin{cases} \mathbf{Z}^{[i]}_{(n[i],1)}(k) = \mathbf{W}^{[i]}_{(n[i],n[i-1])}(k) \cdot \mathbf{Y}^{[i-1]}_{(n[i-1],1)}(k) \\ +\mathbf{B}^{[i]}_{(n[i],1)}(k) \\ \mathbf{Y}^{[i]}_{(n[i],1)}(k) = \sigma^{[i]}\left(\mathbf{Z}^{[i]}_{(n[i],1)}(k)\right) \\ i = 1, 2 \end{cases} \tag{17}$$

$$\begin{cases} \mathbf{Y}^{[i]}_{(n[i],1)}(k) = \mathbf{Z}^{[i]}_{(n[i],1)}(k) \\ = \mathbf{W}^{[i]}_{(n[i],n[i-1])}(k) \cdot \mathbf{Y}^{[i-1]}_{(n[i-1],1)}(k) \\ i = 3 \end{cases} \tag{18}$$

$$\mathbf{Y}^{[0]}_{(2,1)}(k) = \left[i_p{}^*(k) \; i_p(k) \right]^T \tag{19}$$

$$\mathbf{Y}^{[3]}_{(1,1)}(k) = \theta_i{}^*(k) \tag{20}$$

In the initial state, the parameters $\mathbf{B}^{[i]}_{(n[i],1)}(0)$ and $\mathbf{W}^{[i+1]}_{(n[i+1],n[i])}(0)$ need to be initialized randomly. Back propagation and gradient descent are not included and only forward propagation is conducted in this state.

B. MOTION MECHANISM OF THE PROPOSED NN-BASED MTPA CONTROLLER

In the proposed MTPA control system, the continuous action trajectory of BP-NN is shown in Fig. 5. At constant torque $T_e{}^*$, the output of the BP-NN can be adjusted automatically to online-seek the extreme point which is the MTPA point dynamically without pre-training. Specifically, when $\Delta i_p / \Delta \theta_i{}^* > 0$ is valid, the output of BP-NN will be decreased; when $\Delta i_p / \Delta \theta_i{}^* < 0$ is valid, the output of BP-NN will be increased. Ultimately, the operating point of the system will converge to the extreme point and exhibit slight oscillations around the extreme point to dynamically seek the true MTPA point. This process bears a strong resemblance to P&O method, so the proposed method can be considered as an NN-based P&O algorithm.

As a digital controller, the NN-based MTPA controller will eventually be deployed in the discrete domain, such as a DSP controller or a discrete program. Therefore, the discrete motion mechanism between the controller and the motor system needs to be analyzed in detail. Among them, the motor system mainly comprises discrete state-space models of the current PI controller, d-q axis motor equivalent model and speed PI controller. The inputs of the motor system are $i_d{}^*(k)$ and $i_q{}^*(k)$, and the outputs are $i_p{}^*(k+1)$ and $i_p(k+1)$.

The discrete equivalent flowchart of the MTPA point seeking using NN-based P&O algorithm is shown in Fig. 6

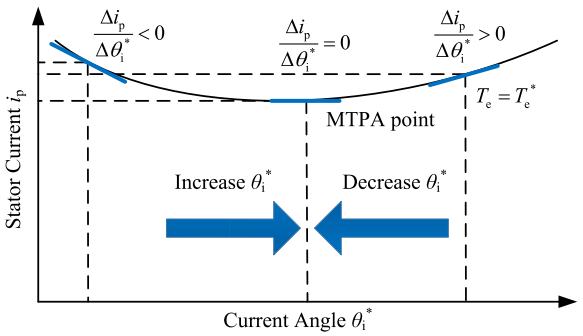

FIGURE 5. Relationship between the MTPA point and its seeking trajectory.

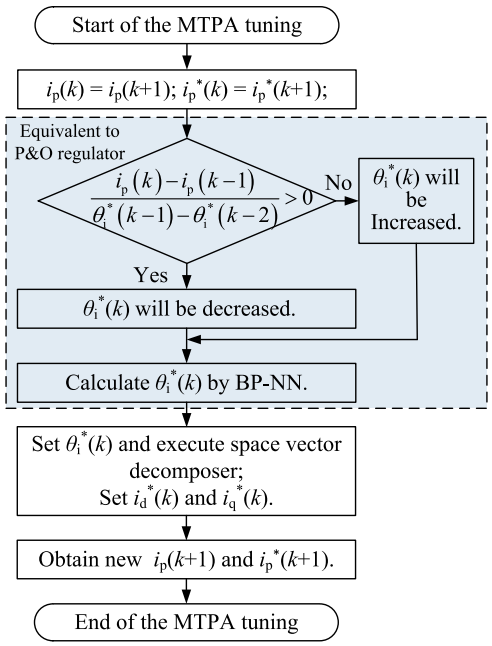

FIGURE 6. Discrete equivalent flowchart of the MTPA point seeking using NN-based P&O algorithm.

at time step k. At the start of MTPA tuning, the actual stator current and stator current reference both obtained from the previous state will be iterative and updated as $i_p(k)$ and $i_p{}^*(k)$. Based on actual stator current and current angle reference in three states, the parameters of BP-NN are updated using back propagation and gradient descent via (13), (14), (15) and (16). This step will result in a positive or negative offset (increase or decrease) of the computed $\theta_i{}^*(k)$ with respect to the actual angle $\theta_i(k)$, where $\theta_i(k)$ corresponds to the $i_p(k)$. This is equivalent to that in the dashed box in Fig. 6. Then, as designed, $i_p(k)$ and $i_p{}^*(k)$ are fed into the BP-NN, and the updated BP-NN is used to compute new $\theta_i{}^*(k)$. This step corresponds to the forward propagation of BP-NN via (17) and (18). Finally, by setting the angle reference $\theta_i{}^*(k)$ to the control system, the stator current $i_p(k+1)$ and stator current reference $i_p{}^*(k+1)$ for the next state can be obtained. This is a complete MTPA tuning process.

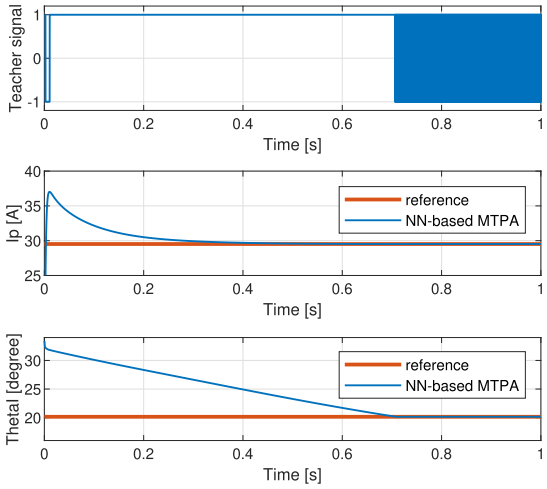

FIGURE 7. Test results of the proposed NN-based MTPA controller.

For example, when the working points are all on the right side of the extreme point, at time step k, the outputs $i_p(k)$ and $\theta_i(k)$ of IPM motor were changed by $\theta_i^*(k-1)$, and the BP-NN with the optimal parameters can be determined based on $i_p(k)$, $i_p(k-1)$, $\theta_i^*(k-1)$ and $\theta_i^*(k-2)$. Since the teacher signal is positive, the $\theta_i^*(k)$ obtained from the input $i_p(k)$ of BP-NN is smaller than $\theta_i(k)$. It will cause the operating point to move left in the convex curve to get closer to the extreme point. In Fig. 7, any operating point from about 0.01 seconds to 0.7 seconds validates the above analysis.

In an unrolling discrete domain, the above iterative process makes the combination of the NN-based MTPA controller and motor system like a recurrent NN, as shown in Fig. 8. The close interaction between two parts in a recurrent manner enables BP-NN to have short-term memory and continuity, and ultimately allows the motor system to converge to the MTPA point instead of getting stuck at arbitrary current angles, as shown in Fig. 7.

IV. SIMULATION AND ANALYSIS

A. FEASIBILITY AND EFFICIENCY ANALYSIS OF THE PROPOSED METHOD AT STEADY STATE

In MATLAB, the state-space average method is used to build the discrete motor model to verify the proposed method, and the main parameters for simulation are shown in Table 2. The conventional MTPA method in section II-B and optimal MTPA method are both used to compare with the proposed NN-based method. The optimal MTPA method can be considered as an ideal MTPA method using real-time and absolutely accurate motor parameters. The copper loss p_c in (5) is used to evaluate the efficiency of different methods. The stator resistance R_s has been measured and determined to be a known constant value.

At steady state, taking the optimal MTPA as a reference (100%), the efficiency comparison between the conventional MTPA using fixed parameters, the optimal MTPA and the proposed NN-based MTPA is shown in Fig. 9, and the steady state comparison between all three methods is shown in Fig. 10.

TABLE 2. Main parameters in the simulation.

Parameter	Value
Load torque, T_{d}	$10\ \mathrm{N}\cdot\mathrm{m}$
Rotational speed, n	2000 rpm
d- and q-axis stator inductances and flux linkage, L_{d}, L_{q}, ψ_{f} (before changing) *	1.20 mH, 2.00 mH, 0.052 Wb
d- and q-axis stator inductances and flux linkage, L_{d}, L_{q}, ψ_{f} (after changing)	1.02 mH, 1.84 mH, 0.039 Wb
Stator resistance, R_{s}	0.343 Ω
Discrete frequency, f_{s}	5 kHz

*Parameters are used for the conventional MTPA controller with fixed parameters.

When the motor parameters remain constant, the conventional MTPA can achieve optimal control due to the use of accurate parameters. In Fig. 10(a) and 10(c), the proposed method has same stator current and current angle as the conventional MTPA and the optimal MTPA. In Fig. 9(a), from efficiency, the copper loss powers of the proposed method and the conventional MTPA are both 100.0% of that of the optimal MTPA. Therefore, the proposed method can track the MTPA point correctly.

When IPM motor undergoes hypothetical variation of parameters, in Fig. 10(b) and 10(d), the conventional MTPA cannot work at the MTPA point due to the use of non-updated parameters. The proposed method has the same stator current and current angle as the optimal MTPA, and can still work at the new MTPA point. In Fig. 9(b), the copper loss power of the conventional MTPA is worse and 100.7% of that of the optimal MTPA. The proposed method has the same efficiency as the optimal MTPA, and has higher efficiency than the conventional MTPA method. We can conclude that the proposed method has true online MTPA tracking capability and does not require motor parameters.

B. FEASIBILITY ANALYSIS UNDER SCENARIOS OF TORQUE AND SPEED VARIATIONS

In the simulated experiment, Fig. 11 and 13 show the feasibility simulations for two different scenarios, respectively. The teacher signal and some parameters of the proposed controller for the two scenarios are shown in Fig. 12 and 14. In both scenarios, the optimal MTPA method is used as a reference for comparison with the proposed NN-based method.

The copper losses of two methods under these two scenarios are shown in Table 3. In the case 1, the average copper loss power of the proposed method is 100.04% of that of the optimal MTPA; in the case 2, the average copper loss power of the proposed method is 100.01% of that of the optimal MTPA. In both scenarios, the power loss error of the two methods is below 0.1%, indicating that the proposed method achieves the same high efficiency as the optimal MTPA control.

Case 1: Under the scenario of torque variation, the load torque undergoes a sudden change every 8 seconds, and increases or decreases by 4 $N\cdot m$ each time. The rotational

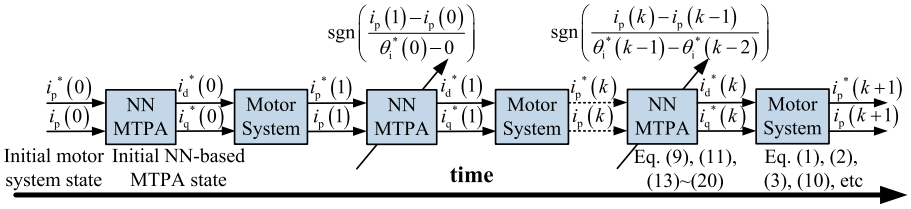

FIGURE 8. MTPA control between the NN-based MTPA controller and motor system in a discrete domain.

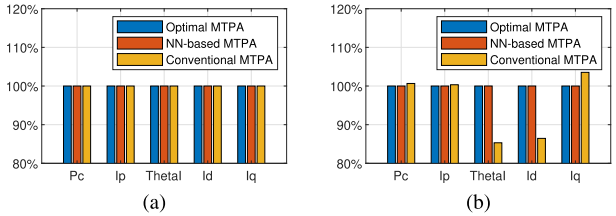

FIGURE 9. Efficiency comparison between the conventional MTPA using fixed parameters, optimal MTPA and proposed NN-based MTPA. (a) Before changing motor parameters. (b) After changing motor parameters.

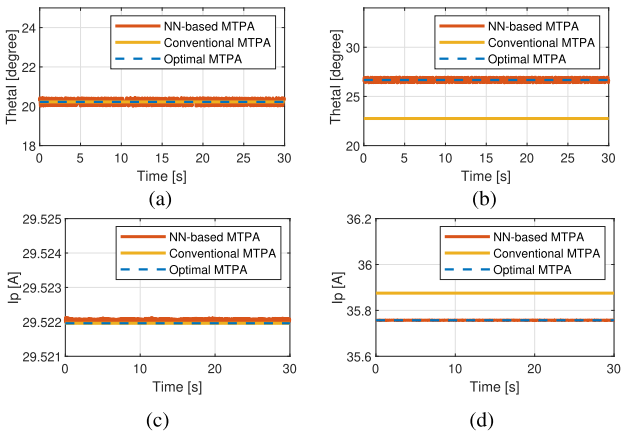

FIGURE 10. Steady state comparison between the conventional MTPA using fixed parameters, optimal MTPA and proposed NN-based MTPA. (a) Current angle before changing motor parameters. (b) Current angle after changing motor parameters. (c) Stator current before changing motor parameters. (d) Stator current after changing motor parameters.

speed command is still 2000 rpm. The rotational speeds, load torques, current angles and stator currents of two methods can be obtained in Fig. 11. From Fig. 11(a), 11(b) and 11(d), under both control methods, the motor system has the same output response in terms of speed, torque and stator current. So, the proposed method can enable stable control. From Fig. 11(c), at steady state, the angle output of the proposed method shows fluctuations, but it aligns with the trend of angle output observed in the optimal MTPA. Moreover, the proposed method is capable of tracking the new different MTPA angle timely under the given periodic torque step disturbances.

In Fig. 12, to remove unfavorable high frequency disturbances, low-pass filters are applied to i_p and θ_i* in the teacher signal. With the introduction of the P&O method, the teacher

TABLE 3. Average copper loss powers of two methods under two scenarios.

Scenarios	Optimal MTPA	NN-based MTPA
case 1	273.50 W	273.61 W
case 2	299.19 W	299.21 W

signal oscillates between positive one and negative one to adjust the current angle dynamically. And after each torque variation, the teacher signal remains consistently positive one or negative one to adjust current angle until entering the new steady state. The parameters of the proposed NN-based controller like weights are convergent, so the proposed method is feasible in this scenario.

Case 2: Under the scenario of speed variation, the rotational speed varies between 1000 rpm and 2000 rpm every 10 seconds, and the load torque remains at 10 $N \cdot m$. The rotational speeds, load torques, current angles and stator currents of two methods are shown in Fig. 13. From Fig. 13(a), 13(b) and 13(d), the proposed method also enables the motor system to output the same response as the optimal MTPA in terms of speed, torque and stator current. From Fig. 13(c), the output angle of the proposed method has a smaller overshoot than the optimal MTPA. When the system is subjected to a constant positive step disturbance in speed at the 10th second, the proposed method exhibits overshoot in the output angle that is at least 50% smaller than the optimal MTPA; when the system is subjected to a constant negative step disturbance in speed at the 20th second, the proposed method's output angle exhibits minimal overshoot compared to the optimal MTPA. Therefore, the proposed method has a good stability.

In Fig. 14, since the torque remains constant at 10 $N \cdot m$, the parameters of the NN-based controller do not show any significant changes in trend, and fluctuate around different constants. The proposed method is convergent and can track the MTPA point under periodic speed step disturbances.

C. TRANSIENT STATOR CURRENT ANALYSIS UNDER SCENARIOS OF TORQUE AND SPEED VARIATIONS

The angle command θ_i output from MTPA controllers will ultimately be reflected in the output stator current i_p of the IPM motor system, where the stator current i_p represents the efficiency of MTPA control methods. Therefore, analyzing the transient stator current can evaluate the transient characteristics of the proposed MTPA controller. The ideal and

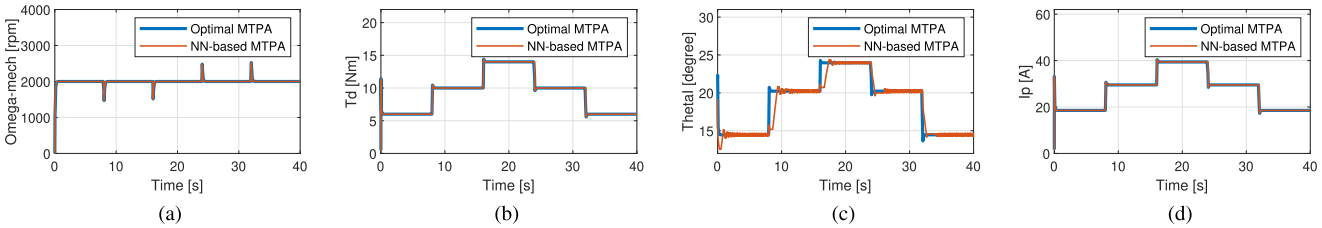

FIGURE 11. NN-based MTPA versus optimal MTPA under the scenario of torque variation. (a) Rotational speed. (b) Load torque. (c) Current angle. (d) Stator current.

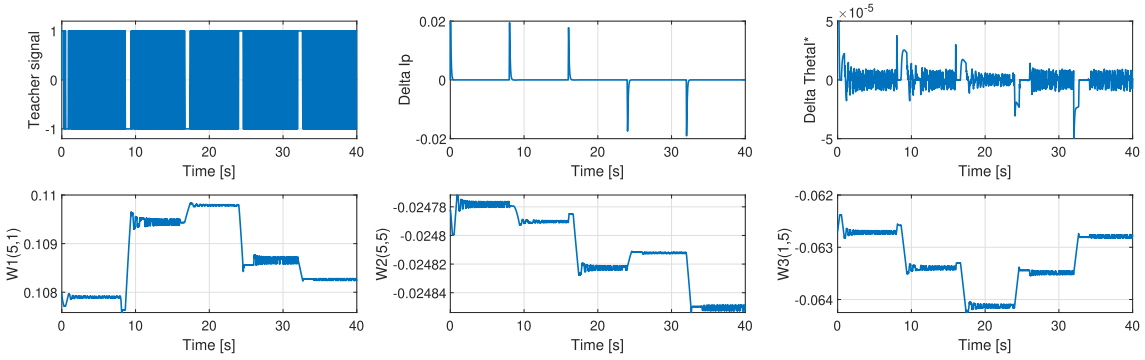

FIGURE 12. Teacher signal and some parameters of the proposed NN-based controller under the scenario of torque variation.

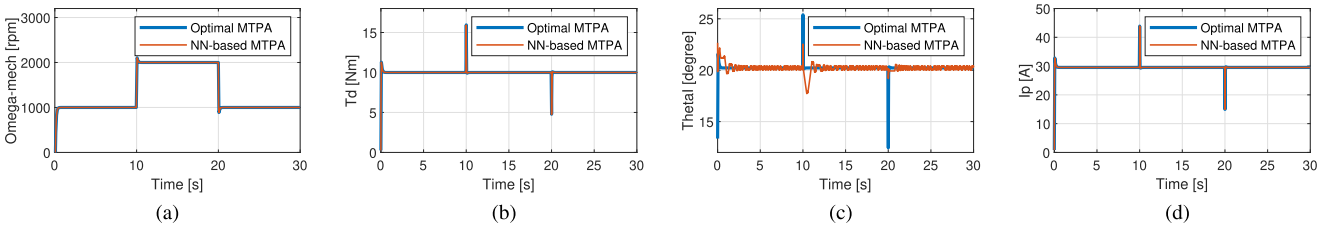

FIGURE 13. NN-based MTPA versus optimal MTPA under the scenario of speed variation. (a) Rotational speed. (b) Load torque. (c) Current angle. (d) Stator current.

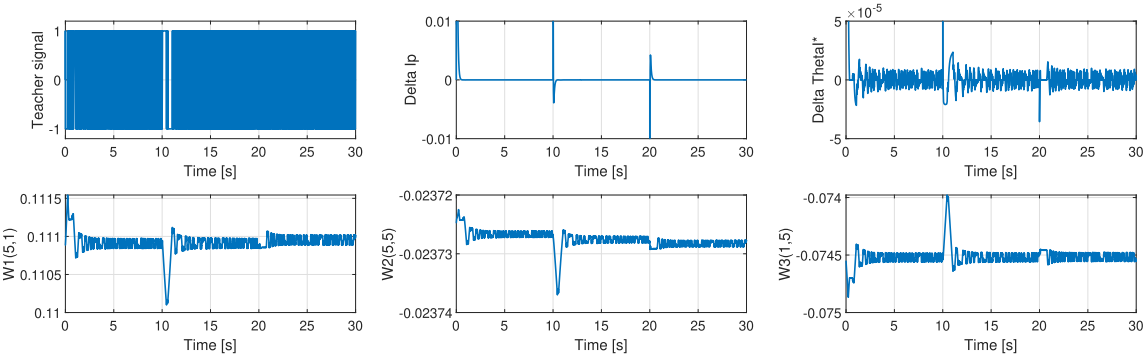

FIGURE 14. Teacher signal and some parameters of the proposed NN-based controller under the scenario of speed variation.

optimal MTPA control is still used for comparison with the proposed method.

Case 1: In this case, the speed remains constant at 2000 rpm. Fig. 15 shows transient stator current responses of the IPM motor system of different torque steps, different torque rises and different torque drops under the optimal MTPA and the proposed MTPA. In Fig. 15(a), under torque step of 10 $N \cdot m$, response times of two methods are about 0.8 and 1.3 seconds, and overshoots of two methods are 24.4% and 24.5%; in Fig. 15(b), under torque step of 8

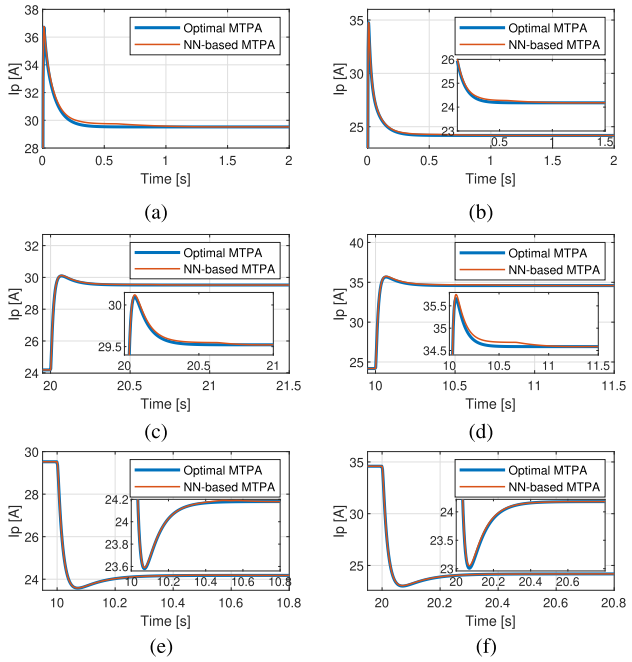

FIGURE 15. Transient stator current responses of the IPM motor system under the optimal MTPA and the proposed MTPA for various torques. (a) Torque step of 10 $N \cdot m$. (b) Torque step of 8 $N \cdot m$. (c) Torque rise from 8 $N \cdot m$ to 10 $N \cdot m$. (d) Torque rise from 8 $N \cdot m$ to 12 $N \cdot m$. (e) Torque drop from 10 $N \cdot m$ to 8 $N \cdot m$. (f) Torque drop from 12 $N \cdot m$ to 8 $N \cdot m$.

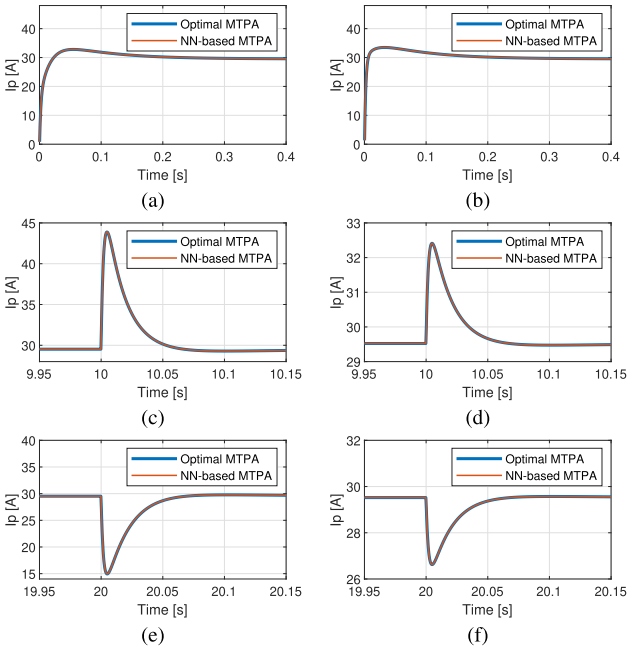

FIGURE 16. Transient stator current responses of the IPM motor system under the optimal MTPA and the proposed MTPA for various speeds. (a) Speed step of 1000 rpm. (b) Speed step of 1600 rpm. (c) Speed rise from 1000 rpm to 2000 rpm. (d) Speed rise from 1600 rpm to 1800 rpm. (e) Speed drop from 2000 rpm to 1000 rpm. (f) Speed drop from 1800 rpm to 1600 rpm.

$N \cdot m$, response times of two methods are about 0.8 and 1.2 seconds, and overshoots of two methods are 43.7% and 43.8%. In Fig. 15(c), under torque rise from 8 $N \cdot m$ to 10 $N \cdot m$ at the 20th second, response times of two methods are about 0.6 and 0.9 seconds, and overshoots of two methods are 1.9% and 2.0%; in Fig. 15(d), under torque rise from 8 $N \cdot m$ to 12 $N \cdot m$ at the 10th second, response times of two methods are about 0.7 and 1.2 seconds, and overshoots of two methods are 3.1% and 3.4%. In Fig. 15(e), under torque drop from 10 $N \cdot m$ to 8 $N \cdot m$ at the 10th second, response times of two methods are about 0.6 and 0.8 seconds, and overshoots of two methods are 2.4% and 2.4%. In Fig. 15(f), under torque drop from 12 $N \cdot m$ to 8 $N \cdot m$ at the 20th second, response times of two methods are about 0.6 and 0.6 seconds, and overshoots of two methods are 4.9% and 4.7%.

From the above results, based on P&O method, the proposed method does not require motor parameters nor an analytical MTPA equation. Therefore, it is sensitive to torque disturbances, which results in a longer time to reach a new steady state point compared to the optimal MTPA. In terms of overshoot, the proposed method exhibits the same good performance as the optimal MTPA. Overall, from stator current profiles in Fig. 15, the proposed method has good transient characteristics.

Case 2: In this case, the load torque remains constant at 10 $N \cdot m$. Transient stator currents under speed steps of 1000 rpm and 1600 rpm are shown in Fig. 16(a) and 16(b), respectively. In Fig. 16(c) and 16(d), transient stator currents corresponding to different speed rises from 1000 rpm to 2000 rpm and from 1600 rpm to 1800 rpm at the 10th second in the IPM motor system can be observed, respectively. In Fig. 16(e) and 16(f), transient stator currents corresponding to speed drops from 2000 rpm to 1000 rpm and from 1800 rpm to 1600 rpm at the 20th second can also be observed, respectively. Obviously, from results in Fig. 16, it can be seen that transient stator currents of the proposed method exhibit the same response time and overshoot as that of the optimal MTPA control. Therefore, the proposed method has the same good transient characteristics as the optimal MTPA control, at constant torque.

V. CONCLUSION

This paper proposed an NN-based online MTPA control method of IPM motor for FOC and sensorless control. The mapping of the loss function to the magnitude of the stator current space vector enables the convergent pursuit of the minimum stator current by the designed BP-NN, which is online trained to minimize the proposed loss function. Based on the online NN technique, the proposed method does not require pre-training for a specific system like offline NN methods, and is easy to process. The analysis of the discrete motion mechanism of the proposed method confirms its resemblance to the characteristics of the P&O technique. Based on the P&O technique, the proposed method does not require any motor parameters or complex model equations.

In the scenario involving given variation of motor parameters, the 0.7% reduction in copper loss confirms that the

proposed method has higher efficiency, compared to the conventional MTPA method with fixed motor parameters. In scenarios involving sudden changes in torque and speed, compared to the optimal MTPA control using real-time and accurate motor parameters, the proposed method has good convergence capability, good stability and good transient characteristics of stator current.

REFERENCES

[1] P. Pillay and R. Krishnan, "Control characteristics and speed controller design for a high performance permanent magnet synchronous motor drive," *IEEE Trans. Power Electron.*, vol. 5, no. 2, pp. 151–159, Apr. 1990, doi: 10.1109/63.53152.

[2] Q. Wang, S. Niu, and T. W. Ching, "A new double-winding Vernier permanent magnet wind power generator for hybrid AC/DC microgrid application," *IEEE Trans. Magn.*, vol. 54, no. 11, pp. 1–5, Nov. 2018, doi: 10.1109/TMAG.2018.2846560.

[3] E. B. Agamloh, "Power and efficiency measurement of motor-variable-frequency drive systems," *IEEE Trans. Ind. Appl.*, vol. 53, no. 1, pp. 766–773, Jan. 2017, doi: 10.1109/TIA.2016.2602807.

[4] F. Tinazzi, P. Sandulescu, L. Peretti, and M. Zigliotto, "On the true maximum efficiency operations of synchronous motor drives," in *Proc. IEEE 12th Int. Conf. Power Electron. Drive Syst. (PEDS)*, Honolulu, HI, USA, Dec. 2017, pp. 1043–1048, doi: 10.1109/PEDS.2017.8289154.

[5] M. Alzayed and H. Chaoui, "Direct voltage MTPA speed control of IPMSM-based electric vehicles," *IEEE Access*, vol. 11, pp. 33858–33871, 2023, doi: 10.1109/ACCESS.2023.3263815.

[6] A. Dianov, N. Kim, Y. Kim, and S. Lim, "Substitution of the universal motor drives with electrolytic capacitorless PMSM drives in home appliances," in *Proc. 9th Int. Conf. Power Electron. ECCE Asia (ICPE-ECCE Asia)*, Seoul, Korea (South), Jun. 2015, pp. 1631–1637, doi: 10.1109/ICPE.2015.7167995.

[7] X. Wu, X. Fu, M. Lin, and L. Jia, "Offline inductance identification of IPMSM with sequence-pulse injection," *IEEE Trans. Ind. Informat.*, vol. 15, no. 11, pp. 6127–6135, Nov. 2019, doi: 10.1109/TII.2019.2932796.

[8] A. Vagati, B. Boazzo, P. Guglielmi, and G. Pellegrino, "Design of ferrite-assisted synchronous reluctance machines robust toward demagnetization," *IEEE Trans. Ind. Appl.*, vol. 50, no. 3, pp. 1768–1779, May 2014, doi: 10.1109/TIA.2013.2284302.

[9] J.-Y. Lee, S.-H. Lee, G.-H. Lee, J.-P. Hong, and J. Hur, "Determination of parameters considering magnetic nonlinearity in an interior permanent magnet synchronous motor," *IEEE Trans. Magn.*, vol. 42, no. 4, pp. 1303–1306, Apr. 2006, doi: 10.1109/TMAG.2006.871951.

[10] Z. Li, D. O'Donnell, W. Li, P. Song, A. Balamurali, and N. C. Kar, "A comprehensive review of state-of-the-art maximum torque per ampere strategies for permanent magnet synchronous motors," in *Proc. 10th Int. Electric Drives Prod. Conf. (EDPC)*, Ludwigsburg, Germany, Dec. 2020, pp. 1–8, doi: 10.1109/EDPC51184.2020.9388199.

[11] A. Dianov and A. Anuchin, "Adaptive maximum torque per ampere control of sensorless permanent magnet motor drives," *Energies*, vol. 13, no. 19, p. 5071, Sep. 2020, doi: 10.3390/en13195071.

[12] F. Tinazzi, S. Bolognani, S. Calligaro, P. Kumar, R. Petrella, and M. Zigliotto, "Classification and review of MTPA algorithms for synchronous reluctance and interior permanent magnet motor drives," in *Proc. 21st Eur. Conf. Power Electron. Appl. (EPE ECCE Europe)*, Genova, Italy, Sep. 2019, p. 10, doi: 10.23919/EPE.2019.8915144.

[13] Y. Miao, H. Ge, M. Preindl, J. Ye, B. Cheng, and A. Emadi, "MTPA fitting and torque estimation technique based on a new flux-linkage model for interior-permanent-magnet synchronous machines," *IEEE Trans. Ind. Appl.*, vol. 53, no. 6, pp. 5451–5460, Nov. 2017, doi: 10.1109/TIA.2017.2726980.

[14] T. Zwerger and P. Mercorelli, "Using a bivariate polynomial in an EKF for state and inductance estimations in the presence of saturation effects to adaptively control a PMSM," *IEEE Access*, vol. 10, pp. 111545–111553, 2022, doi: 10.1109/ACCESS.2022.3215511.

[15] R. F. Schiferl and T. A. Lipo, "Power capability of salient pole permanent magnet synchronous motors in variable speed drive applications," *IEEE Trans. Ind. Appl.*, vol. 26, no. 1, pp. 115–123, Jan. 1990, doi: 10.1109/28.52682.

[16] S. J. Underwood and I. Husain, "Online parameter estimation and adaptive control of permanent-magnet synchronous machines," *IEEE Trans. Ind. Electron.*, vol. 57, no. 7, pp. 2435–2443, Jul. 2010, doi: 10.1109/TIE.2009.2036029.

[17] Y. Zhang, K. Liu, Y. Hu, and S. Yang, "MTPA control of IPMSM with aiding from estimation of dq-axis inductances," in *Proc. IEEE Student Conf. Electric Mach. Syst.*, Huzhou, China, Dec. 2018, pp. 1–5, doi: 10.1109/SCEMS.2018.8624905.

[18] Q. Liu and K. Hameyer, "High-performance adaptive torque control for an IPMSM with real-time MTPA operation," *IEEE Trans. Energy Convers.*, vol. 32, no. 2, pp. 571–581, Jun. 2017, doi: 10.1109/TEC.2016.2633302.

[19] K. Liu, Q. Zhang, J. Chen, Z. Q. Zhu, and J. Zhang, "Online multiparameter estimation of nonsalient-pole PM synchronous machines with temperature variation tracking," *IEEE Trans. Ind. Electron.*, vol. 58, no. 5, pp. 1776–1788, May 2011, doi: 10.1109/TIE.2010.2054055.

[20] S. Bolognani, R. Petrella, A. Prearo, and L. Sgarbossa, "Automatic tracking of MTPA trajectory in IPM motor drives based on AC current injection," *IEEE Trans. Ind. Appl.*, vol. 47, no. 1, pp. 105–114, Jan. 2011, doi: 10.1109/TIA.2010.2090842.

[21] S. Kim, Y.-D. Yoon, S.-K. Sul, and K. Ide, "Maximum torque per ampere (MTPA) control of an IPM machine based on signal injection considering inductance saturation," *IEEE Trans. Power Electron.*, vol. 28, no. 1, pp. 488–497, Jan. 2013, doi: 10.1109/TPEL.2012.2195203.

[22] N. Bedetti, S. Calligaro, C. Olsen, and R. Petrella, "Automatic MTPA tracking in IPMSM drives: Loop dynamics, design, and auto-tuning," *IEEE Trans. Ind. Appl.*, vol. 53, no. 5, pp. 4547–4558, Sep. 2017, doi: 10.1109/TIA.2017.2708683.

[23] T. Sun, J. Wang, and M. Koc, "Virtual signal injection-based direct flux vector control of IPMSM drives," *IEEE Trans. Ind. Electron.*, vol. 63, no. 8, pp. 4773–4782, Aug. 2016, doi: 10.1109/TIE.2016.2548978.

[24] T. Sun, J. Wang, and X. Chen, "Maximum torque per ampere (MTPA) control for interior permanent magnet synchronous machine drives based on virtual signal injection," *IEEE Trans. Power Electron.*, vol. 30, no. 9, pp. 5036–5045, Sep. 2015, doi: 10.1109/TPEL.2014.2365814.

[25] G. Wang, Z. Li, G. Zhang, Y. Yu, and D. Xu, "Quadrature PLL-based high-order sliding-mode observer for IPMSM sensorless control with online MTPA control strategy," *IEEE Trans. Energy Convers.*, vol. 28, no. 1, pp. 214–224, Mar. 2013, doi: 10.1109/TEC.2012.2228484.

[26] E. Daryabeigi, H. Abootorabi Zarchi, G. R. Arab Markadeh, J. Soltani, and F. Blaabjerg, "Online MTPA control approach for synchronous reluctance motor drives based on emotional controller," *IEEE Trans. Power Electron.*, vol. 30, no. 4, pp. 2157–2166, Apr. 2015, doi: 10.1109/TPEL.2014.2323180.

[27] S. Zhao, F. Blaabjerg, and H. Wang, "An overview of artificial intelligence applications for power electronics," *IEEE Trans. Power Electron.*, vol. 36, no. 4, pp. 4633–4658, Apr. 2021, doi: 10.1109/TPEL.2020.3024914.

[28] J. Hao, S. Suo, Y. Yang, Y. Wang, W. Wang, and X. Chen, "Optimization of torque ripples in an interior permanent magnet synchronous motor based on the orthogonal experimental method and MIGA and RBF neural networks," *IEEE Access*, vol. 8, pp. 27202–27209, 2020, doi: 10.1109/ACCESS.2020.2971473.

[29] F.-J. Lin, Y.-T. Liu, and W.-A. Yu, "Power perturbation based MTPA with an online tuning speed controller for an IPMSM drive system," *IEEE Trans. Ind. Electron.*, vol. 65, no. 5, pp. 3677–3687, May 2018, doi: 10.1109/TIE.2017.2762634.

[30] M. T. Hagan, H. B. Demuth, M. H. Beale, and O. De Jesús, *Neural Network Design*, 2nd ed. Boston, MA, USA: Martin Hagan, 2014.

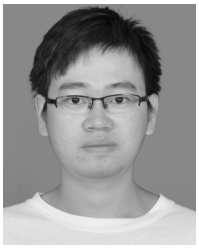

LINFENG SUN received the bachelor's and master's degrees in electrical engineering from Yangzhou University, Yangzhou, China, in 2018 and 2021, respectively. He is currently pursuing the Ph.D. degree with Gunma University, Kiryu, Japan. His current research interests include digital control of power electronics, microgrids, PMSM motor drives, and AI-based control.

JIAWEI GUO received the B.S. degree in electrical engineering from the Changchun University of Science and Technology, in 2020, and the M.S. degree in electrical engineering from Gunma University, Kiryu, Japan, in 2023, where he is currently pursuing the Ph.D. degree. His current research interests include PMSM motor drives, compensation, and AI-based control.

TAKAHIRO KAWAGUCHI (Associate Member, IEEE) received the B.Sc., M.Sc., and Ph.D. degrees in engineering from Keio University, Tokyo, Japan, in 2011, 2013, and 2017, respectively. From 2013 to 2015, he was with the Toshiba Research and Development Center. From 2017 to 2019, he was a Researcher with the Department of Systems and Control Engineering, School of Engineering, Tokyo Institute of Technology, Tokyo. From 2019 to 2020, he was an Assistant Professor with the Department of Systems and Control Engineering, Tokyo Institute of Technology. He is currently an Assistant Professor with the Division of Electronics and Informatics, School of Science and Technology, Gunma University, Gunma, Japan. His current research interests include system identification theory and the application of machine learning techniques. He is a member of the Society of Instrument and Control Engineers and the Institute of System, Control, and Information Engineers.

SEIJI HASHIMOTO (Member, IEEE) received the M.E. and Ph.D. degrees in electrical and electronic engineering from Utsunomiya University, Japan, in 1996 and 1999, respectively. He joined the Department of Mechanical Engineering, Oyama National College of Technology. Since 2002, he has been a Research Associate with the Department of Electronic Engineering, Gunma University, where he is currently a Professor of the Program of Intelligence and Control. He has consulted for companies in control and energy applications and has been a Visiting Professor in China. He has more than 100 refereed articles and more than ten granted and pending patents. His current research interests include system identification, motion control, AI-based control and diagnosis, energy regeneration, and its application to industrial fields. He is currently a member of IEEJ and SICE.

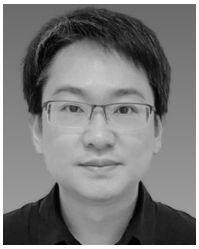

WEI JIANG was born in Yangzhou, China, in 1980. He received the B.S.E.E. degree from Southwest Jiaotong University, Chengdu, China, in 2003, and the M.Sc. and Ph.D. degrees in electrical engineering from The University of Texas at Arlington, TX, in 2006 and 2009, respectively. From 2007 to 2008, he was a Senior Design Engineer with EF Technologies L.L.C., TX, USA. In 2010, he joined Yangzhou University and founded the Smart Energy Laboratory, where he is currently a Professor. He was a Visiting Professor with Gunma University, Japan, in 2012; the University of Strathclyde; and Aston University, U.K., in 2015. He holds two U.S. patents and 15 Chinese patents with two licensed by the industry. His current research interests include digitalized power conditioning to renewable energy and energy storage devices and microscopic analysis of electromechanical energy conversion. He was a recipient of the Yangzhou University Excellent Teaching Award for four times.